Modulation of stability and functionality of a phyto-antioxidant by weakly interacting metal ions: curcumin in aqueous solution

Damayanti Bagchi,[a] Siddhi Chaudhuri,[a] Samim Sardar,[a] Susobhan Choudhury,[a] Nabarun Polley,[a] Peter Lemmens[bc] and Samir Kumar Pal*[a]

The natural polyphenol curcumin and its metal coordinated complexes show obvious benefits in the medical therapies of cancer and several neurodegenerative diseases. On the other side their stability and bioavailability are critical issues. The present study is an attempt to address the stability and functionality of curcumin upon complexation with transition metal ions. We have synthesized and optically characterized metallo–curcumin complexes with Cu(II) and Zn(II). From femtosecond resolved upconversion studies an interaction at the molecular level is revealed based on an observed photoinduced electron transfer from curcumin to the metal ions. In order to investigate the antioxidant activity of the complexes, we have performed a 2,2-diphenyl-1-picrylhydrazyl (DPPH) assay in dark. The Cu(II)–curcumin complex exhibits an enhanced and recyclable activity, more pronounced compared to that of the Zn(II)–curcumin complex, which can be attributed to the weaker O–H bond present in the former case. In contrast, the Zn(II) complex has a higher solubility and stability in aqueous media than the Cu(II) complex. To address stability *vs.* functionality issues, we have suggested a facile method that enhances the solubility and stability of curcumin in aqueous media by metalation with Zn(II) and a successional replacement of Zn(II) in the complex by Cu(II) through a simple route to enhance the activity prior to its use. We have also used the complex in a model anti-bacteriological assay experiment where it shows significantly higher activity compared to pure curcumin. The dichlorofluorescin (DCFH) oxidation indicates an enhancement in ROS generation, which in turn is responsible for the enhanced antioxidative property of the Cu(II)–curcumin complex. Our results provide a promising method to use metallo–curcumin complexes in diverse biological applications.

1. Introduction

Curcumin is a natural yellowish orange diarylheptanoid derived from the rhizomes of *Curcuma longa* L. popularly known as turmeric, a member of the ginger family.[1] The diverse pharmacological applications of curcumin towards various diseases includes Alzheimer's disease,[2] breast cancer,[3] pancreatic cancer,[4] colon cancer,[5] arthritis[6] and oxidative stress induced pathogenesis.[7] Furthermore its promising antioxidant activity[8] anticipates its possible use as a novel drug for other lethal diseases.[9] Curcumin is a linear polyphenol consisting of two *o*-methoxy phenolic groups which are connected by a seven carbon linker consisting of an α,β-unsaturated β-diketo

moiety[10] (Scheme 1a). The diketo group exhibits keto–enol tautomerism (Scheme 1b) and can exist in different types of conformers depending on the nature of the solvent.[11] In most of non-polar and moderately polar solvents, the enol form is generally more stable than the keto form by 5 to 8 kcal mol^{-1} due to strong intramolecular H-bonding.[12] Curcumin is hydrophobic in nature and almost insoluble in water at physiological pH values.[13] This may be due to the presence of β-diketone linkers in the seven carbon chain. This leads to poor bioavailability, limited absorption in body, rapid metabolism and excretion.[14] Therefore it is an important task to improve the bioavailability and solubility of curcumin in water in order to further exploit its medicinal benefits.[15]

To overcome the problem of low bioavailability of curcumin, several methods have been proposed including conjugation to water-soluble polymers[16] or encapsulation in colloidal carriers such as gold nanoparticles,[17] silver nanoparticles[18] and polymer nanoparticles.[19] Recent report suggests that the introduction of dimethylaminomethyl group as substituents on aromatic rings in curcumin improves their aqueous solubility as the basic nitrogen atom will be responsible for converting the target

---

[a]Department of Chemical, Biological and Macromolecular Sciences, S. N. Bose National Centre for Basic Sciences, Block JD, Sector III, Salt Lake, Kolkata 700 098, India. E-mail: skpal@bose.res.in; Fax: +91 033 2335 3477; Tel: +91 033 2335 5706-08
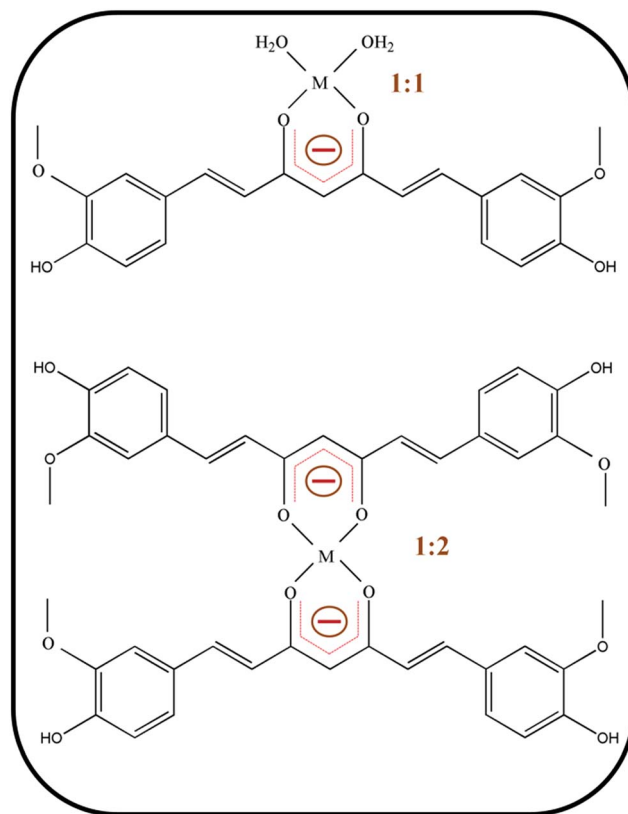*[b]Institute for Condensed Matter Physics, TU Braunschweig, Mendelssohnstraße 3, 38106 Braunschweig, Germany*
[c]Laboratory for Emerging Nanometrology, TU Braunschweig, 38106 Braunschweig, Germany
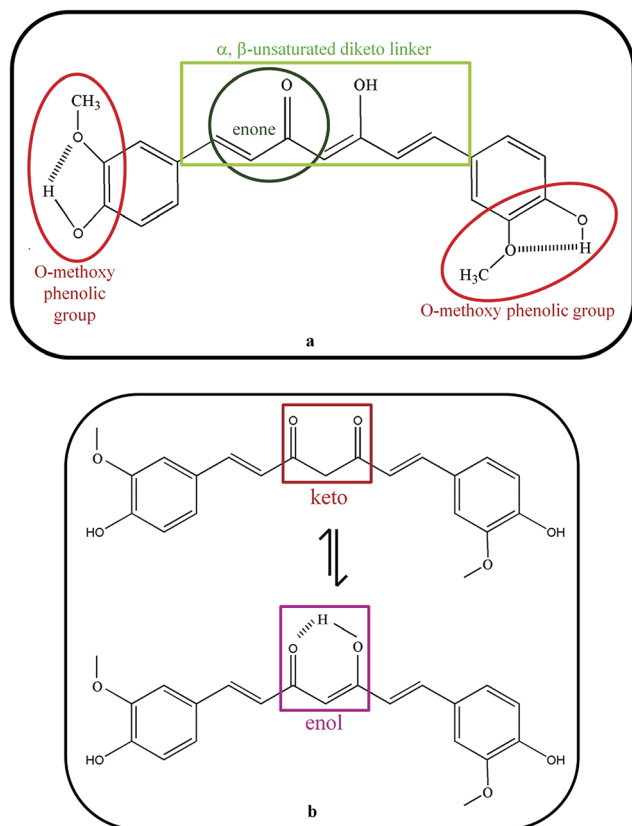
Scheme 1 (a) Structure of curcumin. (b) Keto–enol tautomerism of curcumin.

Scheme 2 Metallo–curcumin complexes.

compounds into the salt forms.[20] Another efficient strategy to improve the bioavailability of curcumin is the formation of complexes with transition metal ions, such as Zn^{2+}, Cu^{2+}, Mn^{2+} and Fe^{2+} which attract interest in the contemporary literature.[21] Some of these complexes are of much higher stability compare to free curcumin.[22] Curcumin acts as a monobasic bidentate ligand in which the α,β-unsaturated β-diketo moiety acts as a chelating agent for complexation with metal ions.[23] Moreover, the stability of curcumin is increased by a factor of 20 after its complexation with Zn(ii) ions at a buffer pH of 7.0.[24] Stable metallo–curcumin complexes are useful in a dual manner: firstly, the complexations increase the drug solubility and can also act as new metal based antioxidants which reduce the cytotoxicity of metal ions.[25] Moreover, complexation of curcumin to palladium(ii) metal centre and its conjugation to another functionalized bioactive ligand, significantly enhance cell-death in prostate cancer cell line through apoptosis signal transduction route due to increased aqueous solubility and hence indicate the possibility of use of metallo–curcumin complexes as potential metal based anti-cancer drugs.[26] Recent studies reveal that deprotonation of the hydroxyl group in the keto–enol moiety leads to the formation of a bidentate β-diketonate which strongly chelates with transitional metal ions namely Cu(ii) and Zn(ii) in two different square planer geometries forming 1 : 1 and 1 : 2 complexes respectively (Scheme 2).[27] Among the different metal bound complexes of curcumin, Zn(ii) and Cu(ii)

complexes received immense importance for their diverse biological applications. The latest studies have shown that the Cu(ii) and curcumin interaction may be important for its anti-cancer[28] and anti-amyloid properties.[29] It has also been reported that due to the reversible electron transfer reactions with superoxide ions, Cu(ii) complexes of curcumin can act as superoxide dismutase enzyme mimics.[30] Zn(ii)–curcumin complexes show anti-cancer, gastro-protective and antidepressant effects and are also very much effective for oxidative stress reduction.[31] These metallo–curcumin complexes are receiving increasing attentions due to their enhanced antioxidant activity. However, the complexes can induce DNA damage due to binding and consequently showing pro-oxidant activity.[32] Therefore, detailed mechanistic investigation of activity of metal complexes is needed. Moreover, both the aqueous solubility and stability are not profoundly altered for a particular metallo–curcumin complex and an alternative approach is required.

In the present study, we have synthesized and optically characterised two metallo–curcumin complexes of Zn(ii) and Cu(ii). Femtosecond resolved fluorescence transient studies of the complexes have clearly unravelled the key time components associated with the excited state electron transfer dynamics. The role of metal ions in antioxidant activity of the complex is evaluated in detail using well-known radical scavenger 2,2-diphenyl-1-picrylhydrazyl (DPPH) for aqueous media in dark condition. Herein, we suggest a new method for both increasing

aqueous solubility by incorporation of Zn(II) and then to enhance the activity, where the metal ion can effectively be altered by Cu(II). Thus, we propose a novel approach in which both stability for storage and activity prior to use can be achieved in aqueous solvent. We have also used the active Cu–curcumin complex in a model bacteriological culture experiment to evaluate the effect of the synthesized complex as an antimicrobial agent. Our studies on ROS marker including dichlorofluorescin (DCFH) in aqueous solution is in consonance with the antibacterial activity of the complex. This study clearly indicates the mechanism of higher free-radical scavenging activity by incorporation of Cu(II) ions in curcumin followed by its action as an antimicrobial agent. The newly suggested method to first increase the water solubility by incorporation of Zn(II) and then replacing it by Cu(II) for higher activity of the metallo–curcumin complex might be useful in future for further *in vivo* experiments.

2. Experimental section

2.1. Materials

In this study analytical grade chemicals without further purification were used for synthesis. Curcumin, $Zn(OAc)_2 \cdot 2H_2O$, $Cu(OAc)_2 \cdot H_2O$, $CuCl_2 \cdot 2H_2O$ were purchased from Sigma-Aldrich. As a suitable solvent for synthesis of metallo–curcumin complexes methanol was used (Merck). Millipore water was used as aqueous solvent. For femtosecond upconversion studies and bacteriological assay dimethyl sulfoxide (DMSO, from Spectrochem) was used as a solvent.

2.2. Synthesis of metallo–curcumin complexes

2.2.1. Zn(II)–curcumin complex. The complex was synthesized by mixing methanolic solution of curcumin with zinc acetate at a molar ratio of 1 : 1.[33] 50 mL of 2 mM methanolic solution of curcumin was prepared and heated at 60 °C for dissolution. Zinc acetate dihydrate (2 mmol) was dissolved in 100 mL methanol by heating. The solution was added into the curcumin solution and a red powder precipitate was produced immediately. The mixture was refluxed for 2 h.[33] The red solid product was filtered and washed firstly by cold methanol and then by water to remove the residue reactants. The purified product was dried in vacuum overnight and the final appearance of the product was a red, crystalline, and solid powder. The synthesized product exhibits 1 : 1 stoichiometric ratio of Zn(II) and curcumin as reported in earlier literature.[21b]

2.2.2. Cu(II)–curcumin complex. The complex was synthesized by the above described procedure only by changing the acetate salt to $Cu(OAc)_2 \cdot H_2O$. The Cu(II)–curcumin was obtained as a dark, brown, crystalline powder. The synthesized Cu complex also shows 1 : 1 stoichiometry as reported in earlier literature.[21b]

2.3. Synthesis of Cu(II)–curcumin complex from Zn(II)–curcumin complex

The synthesized Zn(II)–curcumin complex was dissolved in water by using successive cyclomixing and bath-sonication for 3 h. The solution was centrifuged at 5000 rpm for 5 min and the supernatant (orangish-red) solution was separated. An aqueous solution of $CuCl_2 \cdot 2H_2O$ was added to the collected supernatant solution and vortexed for 2 h. A brown solution was generated.

2.4. Characterization methods

2.4.1. Optical studies. A Shimadzu UV-2600 spectrophotometer was employed to measure absorption spectra using a quartz cell of 1 cm path length. The DPPH degradation kinetics under dark conditions was monitored using the Shimadzu UV-2600 and data were collected at 3 min interval for a total time-window of 30 min. DPPH has a characteristic absorbance maximum at 520 nm. The decrease in this characteristic absorption peak of DPPH was chosen to monitor degradation. Finally, the DPPH absorbance at 520 nm was plotted as a function of time. Steady-state fluorescence measurements were performed using JobinYvon Fluorolog fluorometer. The emissions of all the samples were taken upon excitation at the wavelength of 400 nm. The fluorescence measurements were performed with the excitation and emission bandwidth slits of 5 nm. Femtosecond-resolved fluorescence is measured using a femtosecond upconversion setup (FOG 100, CDP) with full width at half-maximum (FWHM) of 195 fs. The samples were excited at 400 nm, and decay pattern of the emissions were collected at 530 nm. The observed femtosecond resolved decays were fitted using SCIENTIST software. More details of the system can be found in our earlier reports.[34]

2.4.2. Preparation of dichlorofluorescein for *in vitro* measurement of ROS. DCFH was prepared[35] from DCFH-DA (dichlorofluorescindiacetate obtained from Calbiochem) by mixing 0.5 mL of 1.0 mM DCFH-DA in methanol with 2.0 mL of 0.01 N aqueous NaOH at room temperature for 30 min. The mixture was then neutralized with 10 mL of 25 mM NaH_2PO_4, at pH 7.4. This solution was kept on ice in dark until further use.

2.4.3. Bacterial strain and culture conditions. The viable count assay was performed with *E. coli* XL1-Blue cells. The cells were cultured at 37 °C in a liquid Luria–Bertani (LB) medium. When the optical density reached 0.5, the inoculum was serially diluted one lakhs times with the LB medium. Samples of curcumin, Cu(II)–curcumin, Cu(II)-acetate dihydrate and DMSO were added to the diluted culture and incubated for 6 h in dark. The amount of curcumin in Cu(II)–curcumin sample was quantified from the absorption spectra after baseline correction and the absorbance at 430 nm was kept at 0.1 for each samples. The cultures were plated on LB agar plate, and the colonies were counted after overnight incubation.

3. Results & discussion

Metalation of organic ligands causes significant changes in their electronic structures. UV-visible spectroscopy is a useful technique to understand the complexation due to metalation. Fig. 1b shows the absorption maxima of curcumin at 422 nm with a shoulder at 348 nm in water. The absorption peak can be attributed to electronic transition typically a π–π* in nature from (HOMO) to (LUMO) and (HOMO−1) to (LUMO)

respectively.[36] With extensively delocalized π-electrons curcumin exhibits a bright yellow colour (Fig. 1a). After successful attachment of a metal ion to curcumin, a distinct red shift is observed in the absorption spectra. For the Zn(II)–curcumin, a sharp peak was observed at 440 nm, with a small peak at 485 nm. The dark brown Cu(II)–curcumin complex shows more prominent red shift with a broad peak at 512 nm. The red shift may be correlated with the formation of a new, lower energy charge-transfer state by electronic transition from the ligand curcumin to the metal ions. The delocalized π-electron density over the ligand curcumin moiety behaves as a donor to positively charged metal centres with empty d-orbitals behaving as an acceptor, exhibiting a ligand to metal charge transfer band (LMCT).[37] The extent of interaction can be explained on the basis of number of d-electrons present in the system. Zn(II) having a filled d-orbital shows lower interactions compared to

Cu(II), a d[9] system which is prone to be involved in LMCT due to the presence of low-lying empty d orbitals.[27a] Moreover, Fig. 1b demonstrates curcumin and its metal complexes show extended absorbance in near infra-red region. The room temperature PL spectra (Fig. 1c) of curcumin depict a peak at 530 nm upon excitation at 400 nm. However, after metalation with Zn(II) and Cu(II) steady-state emission was significantly decreased although the corresponding absorbance spectra of these solutions are similar. This indicates involvement of non-radiative processes. The inset of Fig. 1c shows excitation spectra of all the samples and a clear quenching is observed. The significant quenching in both emission and excitation spectra suggest internal quenching due to complexation.

Femtosecond resolved fluorescence decay transients of metallo–curcumin samples have been collected to understand the excited state interaction between metal and curcumin. The decay of curcumin was monitored at 530 nm upon excitation at 400 nm, in absence and presence of Cu(II) and Zn(II) in DMSO. The decay profiles are shown in Fig. 2. The fluorescence transient of curcumin is fitted with biexponential decay with lifetime of 3.2 ps (shorter component: signature of solvation dynamics) and 73.5 ps (longer component: indication for excited state intramolecular H atom transfer ESIHT),[38] with an average lifetime of 50.4 ps. The decay profile of curcumin in presence of Cu(II) and Zn(II) show shorter time component of 0.7 ps with an average lifetime of 30.8 ps and 23.0 ps, respectively. The shorter excited state lifetime for Cu(II)–curcumin and Zn(II)–curcumin suggest
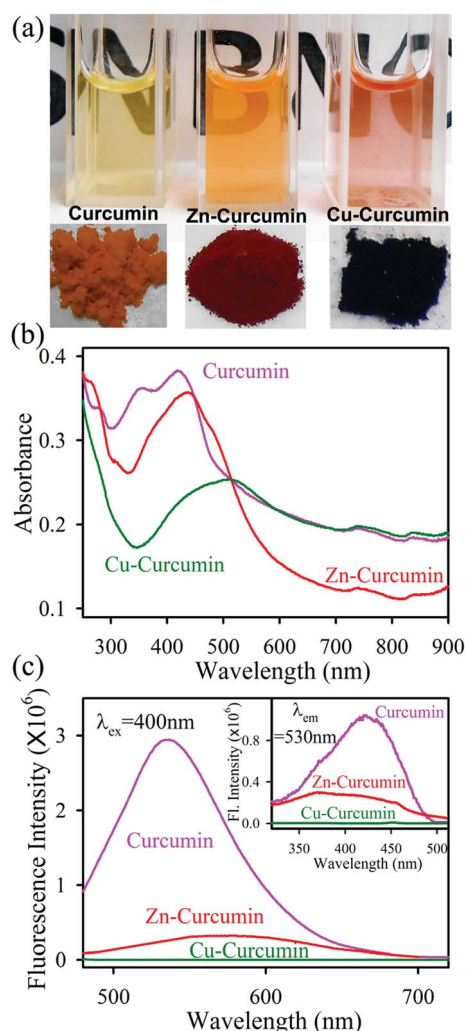

Fig. 1 (a) Photographs of curcumin, Zn–curcumin and Cu–curcumin in water under visible light (b) absorption spectra of curcumin (pink), Zn–curcumin (red), Cu–curcumin (green) (c) room temperature emission spectra of curcumin (pink), Zn–curcumin (red) and Cu–curcumin (green) in water are shown. The excitation wavelength was at 400 nm. Inset shows excitation spectra of curcumin (pink), Zn–curcumin (red) and Cu–curcumin (green).
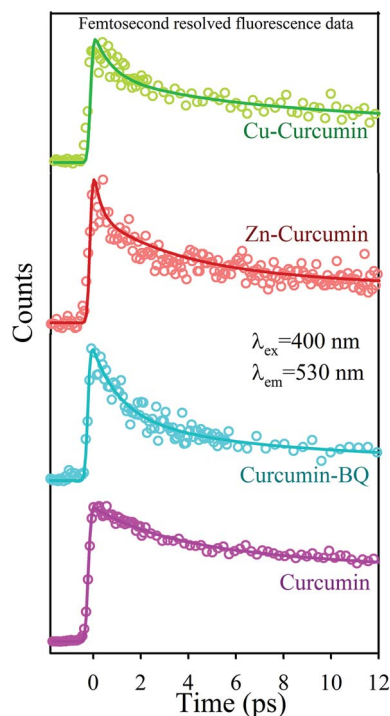

Fig. 2 Femtosecond resolved fluorescence transients of curcumin (pink), curcumin–BQ (cyan), Zn–curcumin (red) and Cu–curcumin (green) in DMSO. Excitation wavelength was at 400 nm and detection wavelength was at 530 nm. The circles are experimental data, and the solid lines are best multiexponential fit.

the photoinduced electron-transfer process from curcumin to metal ions.[27b] In order to confirm the electron migration process, well-known electron acceptor benzoquinone (BQ) has been attached to curcumin. The possible excited state interaction in curcumin–BQ was monitored and the electron transfer timescale (∼0.7 ps) was found to be similar to that of metallo–curcumin samples. It has to be noted that BQ attached curcumin structure might not be similar to that of metallo curcumin complexes but excited state electron transfer timescale is similar due to proximity between two entities in both the cases. Thus, the shorter timescale in presence of metal ions can be rationalized as an electron transfer from curcumin to the attached metal ion. The lifetime components of transients with their relative percentages are presented in a tabular form (Table 1).

The analysis regarding the stability and antioxidant activity of metallo–curcumin complexes in bio-compatible solvent water is essential for application purposes. In this regard, the UV-Vis peak maxima at 430 nm for curcumin in the presence and absence of metal ions were monitored in kinetic mode for 10 min (Fig. 3a) to establish aqueous stability of the complexes. All the solutions under consideration are clear and there is no scattering effect. Zn(II)–curcumin complex shows maximum stability followed by curcumin whereas Cu(II)–curcumin solution shows lowest stability. Fig. 3b demonstrates antioxidant activity of curcumin and metallo–curcumin complexes in dark under stirring condition. Antioxidant activities of the samples are monitored by the decolourization kinetics of stable free radical 2,2-diphenyl-1-picrylhydrazyl (DPPH) in ethanol–water mixture.[39] DPPH, a violet coloured radical is reduced to DPPH$_2$ which is yellow in colour due to donation of an H-atom from the polyphenolic antioxidant to the radical.[40] The absorbance of all the samples is maintained to 0.1 at 430 nm and DPPH is added in such a manner so that the absorbance at 520 nm becomes 0.5 just after addition of DPPH which is much higher compared to self-absorption of the complexes at that particular wavelength. Moreover, the assays were performed under stirring conditions which suggest that there is no decrease in absorbance due to precipitation of the complexes. The free radical quenching kinetics data have been fitted with biexponential decay functions. The time constants are calculated to be 46.5 min, 38.5 min and 6.5 min for curcumin, Zn(II)–curcumin and Cu(II)–curcumin, respectively (Table 2). The increase in the radical scavenging activity for metallo–curcumin samples is clearly evident from Fig. 3b. The enhanced anti-oxidant property for
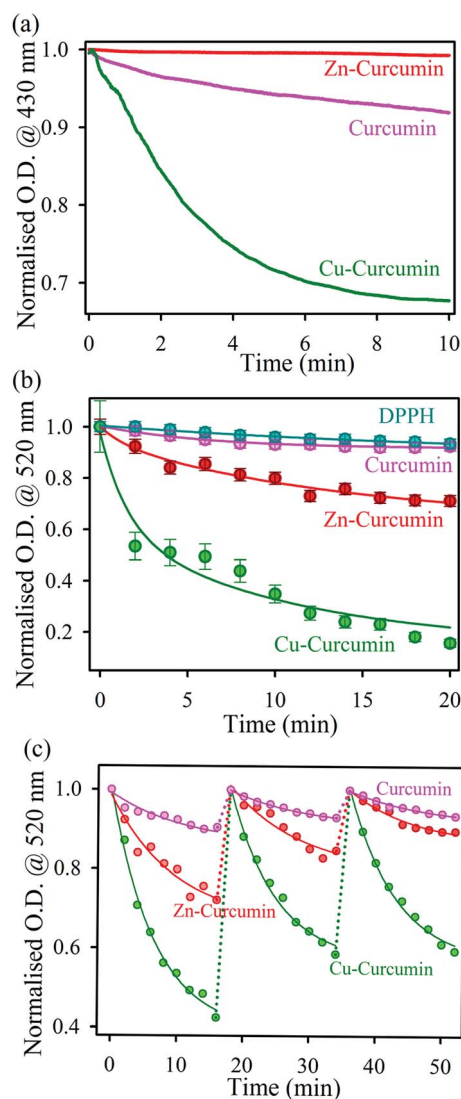

Fig. 3 (a) Stability of curcumin (pink), Zn−curcumin (red) and Cu−curcumin (green) from absorbance at 430 nm in water at 10 min time-window. (b) Depicts the absorption kinetics of DPPH degradation (monitored at 520 nm) in presence of curcumin (pink), Zn−curcumin (red) and Cu−curcumin (green) under stirring condition. The circles are experimental data and the solid lines represent the best biexponential fit with 10% error bar. (c) Cycling curves of DPPH degradation (monitored at 520 nm) in presence of curcumin (pink), Zn−curcumin (red) and Cu−curcumin (green) under stirring condition.

Cu(II)–curcumin can be attributed to weaker ArO–H bond present in o-methoxy phenolic group (red circled in Scheme 1) and a consequent easier H-atom loss process. Due to the presence of stronger O–H bond in case of Zn(II) complex, the radical scavenging activity is many folds lesser compared to Cu(II)-complex.[21b] Furthermore, to confirm the reusability of the highly active radical scavenger Cu(II)–curcumin, recycling experiments have been performed. Three consecutive cycles were conducted (Fig. 3c) which show that the rate of radical scavenging remains almost constant indicating the high activity of Cu(II)–curcumin. Moreover, curcumin and Zn(II)–curcumin complex did not produce any such recyclability. This

Table 1 Femtosecond resolved fluorescence transient data of curcumin and metallo−curcumin samples[a]

Samples	τ_1 (ps)	τ_2 (ps)	τ_3 (ps)	τ_{avg} (ps)
Curcumin	—	3.2 (32.8%)	73.5 (67.2%)	50.4
Cu–curcumin	0.7 (35.5%)	5.0 (25.5%)	75.0 (39.0%)	30.8
Zn–curcumin	0.7 (52.6%)	7.5 (20.5%)	78.9 (26.9%)	23.0
Curcumin–BQ	0.7 (45.5%)	5.0 (38.9%)	75.0 (15.6%)	14.0

[a] The emission (monitored at 530 nm) was detected with 400 nm laser excitation. Numbers in parentheses indicate relative contributions.

Table 2 Time-constants for DPPH degradation in presence of curcumin and metallo−curcumin samples[a]

Samples	t_1 (min)	t_2 (min)	t_{avg} (min)
DPPH	30.0 (25%)	75.0 (75%)	63.8
Curcumin	4.7 (36%)	70.0 (64%)	46.5
Zn−curcumin	4.1 (25%)	50.0 (75%)	38.5
Cu−curcumin	1.5 (46%)	10.8 (54%)	6.5
Zn−curcumin + CuCl$_2$	6.3 (27%)	9.1 (73%)	8.3

[a] Numbers in parentheses indicate relative contributions.

observation suggests that only for Cu(II)−curcumin complex, radical scavenging activity become rejuvenated after each cycle. Fig. 3c depicts that in the first cycle, the scavenging activity (57% DPPH degradation) is obtained in the presence of a very small amount of Cu(II)−curcumin (OD at 430 nm = 0.1), and the degradation become 41% after third cycle. The time constants are shown in Table 3. The results demonstrate that Cu(II)−curcumin serve as a highly effective recyclable free-radical scavenger than Zn(II)−curcumin and curcumin in water.

From Fig. 3, it is clear that Zn(II)−curcumin complex is more stable in water whereas the less stable Cu(II)−curcumin is more active. In order to clarify this issue, an alternative approach is followed. Before using as an antioxidant more stable Zn−curcumin should be kept for greater aqueous stability and then addition of CuCl$_2$·2H$_2$O followed by vortex for 2 h can replace Zn(II) by Cu(II) which eventually enhances the activity. Fig. 4a illustrate the visible colour change by addition of CuCl$_2$·2H$_2$O in Zn(II)-complex from orange to brown, indicating formation of Cu(II)-complex. Fig. 4b shows the UV-Vis spectra of Zn−curcumin after addition of CuCl$_2$ solution, which is distinctly different from Zn(II)−curcumin and CuCl$_2$·2H$_2$O (data not shown) and more likely to the absorbance spectra of Cu(II)−curcumin complex. To evaluate the antioxidant properties, DPPH degradation kinetics was monitored. Fig. 4c indicates that there is a clear increase in antioxidant property compared to Zn−curcumin and CuCl$_2$·2H$_2$O (data not shown). The time constant is calculated to be 8.3 min (fitted with biexponential

function) for the complex which is comparable to that of Cu(II)−curcumin (Table 2). This result is in agreement with the fact that Cu(II) has higher affinity for complexation than Zn(II), due to d-electron density distribution.[36] Altogether, Fig. 4 suggests a simple methodology for both the enhancement of aqueous stability and antioxidant property in metallo−curcumin complexes.

In the view to investigate the anti-microbial action, highly active Cu(II)−curcumin was used as a potential antibacterial agent in dark for the inhibition of growth of *Escherichia coli* (*E. coli*). The upper panel of Fig. 5 shows picture of *E. coli* cultures treated with DMSO, Cu(OAc)$_2$·H$_2$O, curcumin and Cu(II)−curcumin in dark. The inhibition in growth of the bacterial culture for Cu(II)-complex is clearly visible. The culture treated with Cu(II)−curcumin complex contains a smaller number of colonies with respect to the control samples and
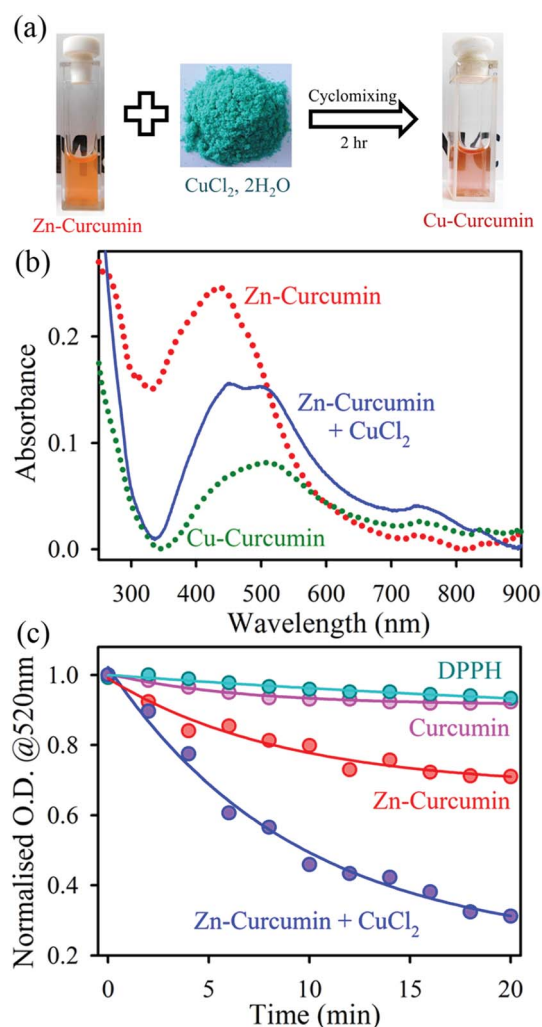

Fig. 4 (a) Pictorial representation of Cu replacement in Zn−curcumin which leads to formation of Cu−curcumin. (b) Absorption spectra of Zn−curcumin (red dotted), Cu−curcumin (green dotted) and Zn−curcumin + CuCl$_2$ (blue solid line) (c) shows the kinetics of DPPH degradation (monitored at 520 nm) in presence of curcumin (pink), Zn−curcumin (red) and Zn−curcumin + CuCl$_2$ (blue) under stirring condition.

Table 3 DPPH degradation efficiency data for cycling curves in presence of curcumin and metallo−curcumin samples[a]

Sample	Cycle	t_1 (min)	t_2 (min)	t_{avg} (min)	Degradation percentage (%)
			Efficiency		
Curcumin	1st	6.8 (28.6%)	70.0 (71.4%)	52.0	11.0
	2nd	7.8 (29.4%)	70.5 (70.6%)	52.1	7.0
	3rd	6.5 (28.6%)	71.0 (71.4%)	52.6	6.0
Zn−curcumin	1st	4.6 (26.0%)	50.3 (74.0%)	38.5	28.0
	2nd	33.7 (80.4%)	45.1 (19.6%)	36.0	15.0
	3rd	4.1 (18.0%)	51.0 (82.0%)	42.6	10.0
Cu−curcumin	1st	6.6 (50.0%)	6.6 (50.0%)	6.6	57.0
	2nd	6.9 (5.0%)	9.9 (95.0%)	9.8	41.0
	3rd	9.0 (50.0%)	9.0 (50.0%)	9.1	41.0

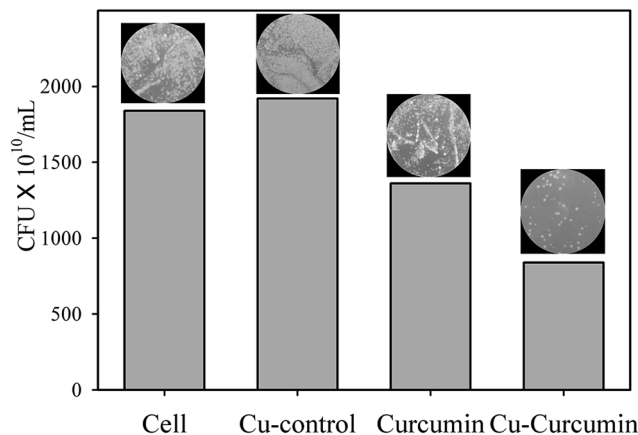[a] Numbers in parentheses indicate relative contributions.

Fig. 5 Bacteriological assay of cell, Cu-control, curcumin and Cu–curcumin in dark. The upper panel shows images of *E. coli* plates in presence of the corresponding samples.
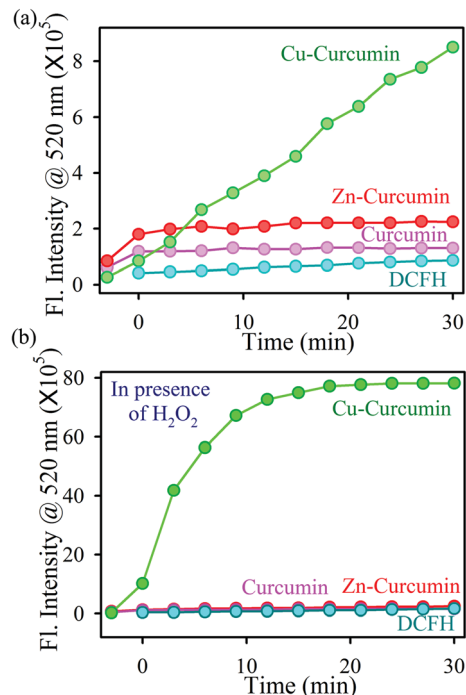

Fig. 6 (a) The DCFH oxidation (monitored at 520 nm) with time in presence of curcumin (pink), Zn–curcumin (red) and Cu–curcumin (green) and DCFH only (cyan) in water under dark condition. The excitation was at 488 nm. (b) The DCFH oxidation in presence of H_2O_2 (monitored at 520 nm) with the samples of curcumin (pink), Zn–curcumin (red) and Cu–curcumin (green) and DCFH only (cyan) in water under dark condition. The excitation was at 488 nm.

cultures containing curcumin and $Cu(OAc)_2$. In control and $Cu(OAc)_2$ treated samples, the colony forming units (CFU) are almost similar. In case of curcumin treated samples, the bacterial growth was inhibited to 35% whereas maximum inhibition is obtained for Cu(II)–curcumin treated samples. The decrease of CFU is 60%. In order to explain the detailed mechanistic view of both antioxidant and antimicrobial action of Cu(II)–curcumin complex, the ROS generation was investigated directly by dichlorofluorescin–dichlorofluorescein (DCFH–DCF) conversion in aqueous medium. Nonfluorescent DCFH is a well-known ROS marker, which is oxidized to fluorescent DCF in presence of ROS.[41] The emission intensity at 520 nm of DCF was monitored with time to evaluate the extent of ROS generation. Fig. 6a shows that there is maximum increase in fluorescence intensity in presence of Cu(II)–curcumin complex. Moreover no significant enhancement of fluorescence intensity was observed for both curcumin and its Zn(II) complex. To confirm the ROS generation, H_2O_2, which is a proper electron acceptor can act as a source of OH[•] radical was added to the system. This results in a huge enhancement of fluorescence intensity in case of the Cu(II)–curcumin complex (Fig. 6b). The enhancement of ROS formation can be anticipated with the chain reaction in presence of H_2O_2.[42] The antioxidant effect of ROS generator Cu(II)–curcumin can be explained by the fact that the ROS influence the activity of electron releasing substituents present in the phenolic antioxidant like Cu(II)–curcumin (ArOH). This results in breaking of the O–H bond and release of hydrogen radical as reported in the earlier literature.[9a,43] The hydrogen radicals can react with nucleophilic free-radicals like DPPH and quench their activity as shown in the following equation.

$$\text{ArOH} + \text{X}^{\bullet} = \text{ArO}^{\bullet} + \text{XH} \ (\text{X}^{\bullet} = \text{DPPH}^{\bullet})$$
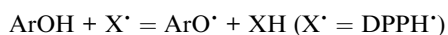
Thus Cu(II)–curcumin can act as a ROS generator as well as the by-product during ROS generation (H[•]) can quench the free radicals to show antioxidant activity.

4. Conclusion

We have synthesized and optically characterized the metallo–curcumin complexes of Cu(II) and Zn(II). The femtosecond resolved upconversion technique confirms excited state electron transfer processes from the ligand curcumin to the metal ions. 2,2-Diphenyl-1-picrylhydrazyl (DPPH) assay in dark proved the enhanced antioxidant property of curcumin by incorporation of Cu(II) ion. The rejuvenating antioxidant properties of Cu(II)–curcumin have been illustrated, which reveal recyclability and highly efficient antioxidant property of the complex. Moreover, the complex shows greater antimicrobial effect for the inhibition of *E. coli* growth compared to that of free curcumin. To get a more detailed mechanistic view, we performed dichlorofluorescin (DCFH) oxidation, which clearly shows ROS generation is more in case of Cu(II)–curcumin complexes. These results suggest that the presence of ROS induces the O–H bond breaking which is responsible for showing free-radical scavenging activity. Thus, the Cu(II)–curcumin complex behaves both as an anti-oxidant and anti-microbial agent. Moreover, to take care of both the factor of stability and activity of metallo–curcumin complexes, we propose a new method where aqueous stability is enhanced by Zn(II) complex and the activity can be increased by replacing Zn(II) with Cu(II) through a simple route prior to its use. The shift in absorbance spectra clearly demonstrates the replacement of metal ion at the reaction site.
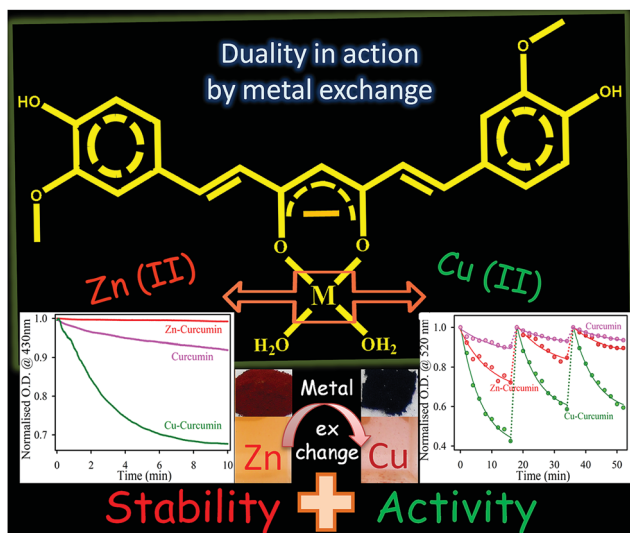
Scheme 3 Schematic representation of metal exchange process leading to duality in action: enhancement of both aqueous stability and anti-oxidant property.

The overall observation is schematically represented in Scheme 3. We believe that our study will effectively lead to the development of multifunctional, stable metallo–curcumin complexes having excellent potential to be used for *in vivo* studies and as future medicines.

Acknowledgements

References

1 B. B. Aggarwal, A. Kumar and A. C. Bharti, *Anticancer Res.*, 2003, **23**, 363–398.

2 (*a*) F. Yang, G. P. Lim, A. N. Begum, O. J. Ubeda, M. R. Simmons, S. S. Ambegaokar, P. P. Chen, R. Kayed, C. G. Glabe, S. A. Frautschy and G. M. Cole, *J. Biol. Chem.*, 2005, **280**, 5892–5901; (*b*) T. Jiang, G.-R. Zhou, Y.-H. Zhang, P.-C. Sun, Q.-M. Du and P. Zhou, *RSC Adv.*, 2012, **2**, 9106–9113.

3 C. D. Mock, B. C. Jordan and C. Selvam, *RSC Adv.*, 2015, **5**, 75575–75588.

4 (*a*) K. I. Priyadarsini, *Molecules*, 2014, **19**, 20091–20112; (*b*) M. Salem, S. Rohani and E. R. Gillies, *RSC Adv.*, 2014, **4**, 10815–10829.

5 M. Tan, J. Luo and Y. Tian, *RSC Adv.*, 2014, **4**, 61948–61959.

6 T. Esatbeyoglu, P. Huebbe, I. M. Ernst, D. Chin, A. E. Wagner and G. Rimbach, *Angew. Chem., Int. Ed. Engl.*, 2012, **51**, 5308–5332.

7 J. Wang, H. Wang, R. Zhu, Q. Liu, J. Fei and S. Wang, *Biomaterials*, 2015, **53**, 475–483.

8 L. R. Barclay, M. R. Vinqvist, K. Mukai, H. Goto, Y. Hashimoto, A. Tokunaga and H. Uno, *Org. Lett.*, 2000, **2**, 2841–2843.

9 (*a*) G. Litwinienko and K. U. Ingold, *J. Org. Chem.*, 2004, **69**, 5888–5896; (*b*) S. V. Jovanovic, C. W. Boone, S. Steenken, M. Trinoga and R. B. Kaskey, *J. Am. Chem. Soc.*, 2001, **123**, 3064–3068.

10 B. B. Aggarwal and B. Sung, *Trends Pharmacol. Sci.*, 2009, **30**, 85–94.

11 K. I. Priyadarsini, *Curr. Pharm. Des.*, 2013, **19**, 2093–2100.

12 L. Nardo, R. Paderno, A. Andreoni, M. Másson, T. Haukvik and H. H. Tønnesen, *Spectroscopy*, 2008, **22**, 187–198.

13 K. Bairwa, J. Grover, M. Kania and S. M. Jachak, *RSC Adv.*, 2014, **4**, 13946–13978.

14 P. Basnet and N. Skalko-Basnet, *Molecules*, 2011, **16**, 4567–4598.

15 H. Hatcher, R. Planalp, J. Cho, F. M. Torti and S. V. Torti, *Cell. Mol. Life Sci.*, 2008, **65**, 1631–1652.

16 C. Banerjee, S. Maiti, M. Mustafi, J. Kuchlyan, D. Banik, N. Kundu, D. Dhara and N. Sarkar, *Langmuir*, 2014, **30**, 10834–10844.

17 D. K. Singh, R. Jagannathan, P. Khandelwal, P. M. Abraham and P. Poddar, *Nanoscale*, 2013, **5**, 1882–1893.

18 S. Kundu and U. Nithiyanantham, *RSC Adv.*, 2013, **3**, 25278–25290.

19 S. Bisht, G. Feldmann, S. Soni, R. Ravi, C. Karikar, A. Maitra and A. Maitra, *J. Nanobiotechnol.*, 2007, **5**, 1–18.

20 X. Fang, L. Fang, S. Gou and L. Cheng, *Bioorg. Med. Chem. Lett.*, 2013, **23**, 1297–1301.

21 (*a*) S. Wanninger, V. Lorenz, A. Subhan and F. T. Edelmann, *Chem. Soc. Rev.*, 2015, **44**, 4986–5002; (*b*) X.-Z. Zhao, T. Jiang, L. Wang, H. Yang, S. Zhang and P. Zhou, *J. Mol. Struct.*, 2010, **984**, 316–325; (*c*) T. M. Kolev, E. A. Velcheva, B. A. Stamboliyska and M. Spiteller, *Int. J. Quantum Chem.*, 2005, **102**, 1069–1079; (*d*) S. Sardar, S. Sarkar, M. T. Myint, S. Al-Harthi, J. Dutta and S. K. Pal, *Phys. Chem. Chem. Phys.*, 2013, **15**, 18562–18570; (*e*) P. Kar, S. Sardar, E. Alarousu, J. Sun, Z. S. Seddigi, S. A. Ahmed, E. Y. Danish, O. F. Mohammed and S. K. Pal, *Chem.–Eur. J.*, 2014, **20**, 10475–10483.

22 D. Pucci, A. Crispini, B. S. Mendiguchia, S. Pirillo, M. Ghedini, S. Morelli and L. De Bartolo, *Dalton Trans.*, 2013, **42**, 9679–9687.

23 E. Ferrari, R. Benassi, S. Sacchi, F. Pignedoli, M. Asti and M. Saladini, *J. Inorg. Biochem.*, 2014, **139**, 38–48.

24 B. Zebib, Z. Mouloungui and V. Noirot, *Bioinorg. Chem. Appl.*, 2010, **2010**, 292760.

25 S. Daniel, J. L. Limson, A. Dairam, G. M. Watkins and S. Daya, *J. Inorg. Biochem.*, 2004, **98**, 266–275.

26 A. Valentini, F. Conforti, A. Crispini, A. De Martino, R. Condello, C. Stellitano, G. Rotilio, M. Ghedini, G. Federici, S. Bernardini and D. Pucci, *J. Med. Chem.*, 2009, **52**, 484–491.

27 (*a*) M. A. Addicoat, G. F. Metha and T. W. Kee, *J. Comput. Chem.*, 2011, **32**, 429–438; (*b*) M. H. Leung, D. T. Pham, S. F. Lincoln and T. W. Kee, *Phys. Chem. Chem. Phys.*, 2012, **14**, 13580–13587.

28 V. D. John, G. Kuttan and K. Krishnankutty, *J. Exp. Clin. Cancer Res.*, 2002, **21**, 219–224.

29 L. Rossi, S. Mazzitelli, M. Arciello, C. R. Capo and G. Rotilio, *Neurochem. Res.*, 2008, **33**, 2390–2400.

30 A. Barik, B. Mishra, A. Kunwar, R. M. Kadam, L. Shen, S. Dutta, S. Padhye, A. K. Satpati, H. Y. Zhang and K. Indira Priyadarsini, *Eur. J. Med. Chem.*, 2007, **42**, 431–439.

31 X. Mei, D. Xu, S. Xu, Y. Zheng and S. Xu, *Chem.–Biol. Interact.*, 2012, **197**, 31–39.

32 H. Ahsan, N. Parveen, N. U. Khan and S. M. Hadi, *Chem.–Biol. Interact.*, 1999, **121**, 161–175.

33 R. Hariharan, S. Senthilkumar, A. Suganthi and M. Rajarajan, *Mater. Res. Bull.*, 2012, **47**, 3090–3099.

34 (*a*) R. Saha, P. K. Verma, S. Rakshit, S. Saha, S. Mayor and S. K. Pal, *Sci. Rep.*, 2013, **3**, 1580; (*b*) S. Choudhury, P. K. Mondal, V. K. Sharma, S. Mitra, V. G. Sakai, R. Mukhopadhyay and S. K. Pal, *J. Phys. Chem. B*, 2015, 10849–10857.

35 S. Sardar, S. Chaudhuri, P. Kar, S. Sarkar, P. Lemmens and S. K. Pal, *Phys. Chem. Chem. Phys.*, 2015, **17**, 166–177.

36 G. B. Kaufman, *J. Chem. Educ.*, 1993, **70**, A279.

37 A. Giri, N. Goswami, C. Sasmal, N. Polley, D. Majumdar, S. Sarkar, S. N. Bandyopadhyay, A. Singha and S. K. Pal, *RSC Adv.*, 2014, **4**, 5075–5079.

38 R. Adhikary, P. Mukherjee, T. W. Kee and J. W. Petrich, *J. Phys. Chem. B*, 2009, **113**, 5255–5261.

39 S. Chaudhuri, S. Batabyal, N. Polley and S. K. Pal, *J. Phys. Chem. A*, 2014, **118**, 3934–3943.

40 S. Chaudhuri, S. Sardar, D. Bagchi, S. S. Singha, P. Lemmens and S. K. Pal, *J. Phys. Chem. A*, 2015, **119**, 4162–4169.

41 C. P. LeBel, H. Ischiropoulos and S. C. Bondy, *Chem. Res. Toxicol.*, 1992, **5**, 227–231.

42 J. Nakamura, E. R. Purvis and J. A. Swenberg, *Nucleic Acids Res.*, 2003, **31**, 1790–1795.

43 P. Malik and T. K. Mukherjee, *Chin. J. Biol.*, 2014, **2014**, 396708.